Design of a Biologically-Inspired Underwater Burrowing Robot with On-Board Actuation

by

Daniel S. Dorsch

S.B., Massachusetts Institute of Technology (2012)

Submitted to the Department of Mechanical Engineering
in partial fulfillment of the requirements for the degree of

Master of Science in Mechanical Engineering

at the

MASSACHUSETTS INSTITUTE OF TECHNOLOGY

February 2015

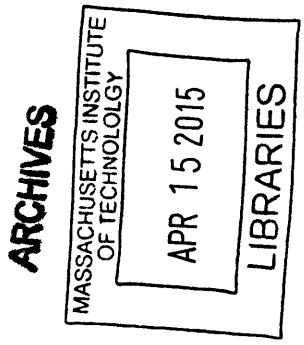

Author ..... Signature redacted ....
Department of Mechanical Engineering
January 16, 2015

Certified by ..... Signature redacted .....
Amos G. Winter V
Assistant Professor of Mechanical Engineering
Thesis Supervisor

Accepted by ..... Signature redacted
David E. Hardt
Professor of Mechanical Engineering

Design of a Biologically-Inspired Underwater Burrowing Robot with On-Board Actuation

by

Daniel S. Dorsch

Submitted to the Department of Mechanical Engineering
on January 16, 2015, in partial fulfillment of the
requirements for the degree of
Master of Science in Mechanical Engineering

Abstract

The Atlantic razor clam (Ensis *directus*) burrows by contracting its valves, fluidizing the surrounding soil and reducing burrowing drag. Moving through a fluidized, rather than static, soil requires energy that scales linearly with depth, rather than depth squared. In addition to providing an advantage for the animal, localized fluidization may provide significant value to engineering applications such as vehicle anchoring and underwater pipe installation. This thesis presents the design of RoboClam 2, a self-actuated, radially expanding burrowing mechanism that utilizes E. *directus* burrowing methods. The device is sized to be a platform for an anchoring system for autonomous underwater vehicles. The scaling relationships necessary for the creation of this internally actuated burrowing robot are presented. These relationships allow for designing devices of different sizes for other applications, and describe optimal sizing and power needs for various size subsea burrowing systems. RoboClam 2 is a proof of concept iteration of a digging mechanism that utilizes localized fluidization. It will be used for testing digging parameters in a laboratory setting and validating the theory presented.

Thesis Supervisor: Amos G. Winter V
Title: Assistant Professor of Mechanical Engineering

Acknowledgments

There are many people who have helped with this project. Without them, this work would not have been possible and I am very grateful for their support and advice during this project and while at MIT. The community is truly amazing. Everyone I meet is very supportive, encouraging, and passionate.

- I am very thankful to Amos for his mentoring during this project and my work with him over the last six years. Without his encouragement, I would likely not have gone to grad school. I am also thankful for the freedom I have had to work on other projects at the same time, and I am excited to see how the new MakerWorks space we are establishing will influence Mechanical Engineering at MIT.

- Without the support from Bluefin Robotics, this project would not have been possible. It has been great working with them, and I look forward to seeing what happens with this technology under their development.

- My family has been instrumental in getting me to where I am today. They have supported me every step of the way in life, and during college and graduate school and without them I would not be where I am today.

- I am very lucky to have such great friends at MIT who always have my back. They are what makes the hard times easier to get through, and make graduate school a lot of fun, even when it is a lot of work.

- My labmates are awesome and I am glad we have such an amazing group of people working together. It is a fun relationship where we work together as coworkers, but also spend time together as friends.

- I am especially thankful to Natasha for the support and encouragement she provides. I am very lucky to be working in the same lab and have enjoyed spending time together.

- I am very thankful to the following five people, Raghav Aggarwal, Josh Wiens, Murthy Arelekatti, Aaron Ramirez, and Kerstin Nordstrom for their help with different parts of this project.

- The representatives at LinMot have been especially helpful with this project. They have provided amazing support for my questions and issues while getting the linear actuator working.

- I am thankful for the NSF and their support of me as a graduate student through the Graduate Research Fellows Program

Contents

List of Figures

List of Tables

Chapter 1

Introduction

1.1 Motivation

There are many applications in which attaching to the seafloor is beneficial. This can be accomplished by burrowing into the soil, and many animals have found methods to do so. While some animals, such as crabs, create burrows, others use methods that allow them to move more efficiently through the soil, by propagating cracks [1] or wiggling like a snake [2].

There are many different systems that can benefit from improved burrowing and anchoring technologies. Anchoring autonomous underwater vehicles (AUVs) is one example. Improved anchors could also be used for anchoring larger equipment, such as ships, oil recovery equipment, or repositionable buoys. Lower energy, more efficient systems could reduce the weight needed for an anchor and increase the number of devices that could efficiently use an anchor. For example, current medium sized AUVs do not carry a conventional anchor, as it would be too heavy to use and difficult to retrieve once deployed [3]. A system that is lightweight and could easily detach from the seafloor when desired would be beneficial in this application.

1.2 Understanding of Ensis directus

The Atlantic razor clam, Ensis *directus*, exhibits a unique method for burrowing into soil (Fig. 1-1). This animal is small, about 20 cm (8 inches) long and 3.2 cm (1.25 inches) wide [4]. It consists of two shell halves that move about a hinge on one side. The shell is spring loaded to open, and muscles cause the shell to close. E. *directus* is fairly weak; its foot can produce about 10 N of pulling force, which should only be enough to pull the animal into packed soil 1-2 cm. In reality, razor clams inhabit soil up to 70 cm deep [5]. They reach this depth by fluidizing the soil around them to reduce drag. It is this ability that makes E. *directus* of interest for a low energy anchoring system.

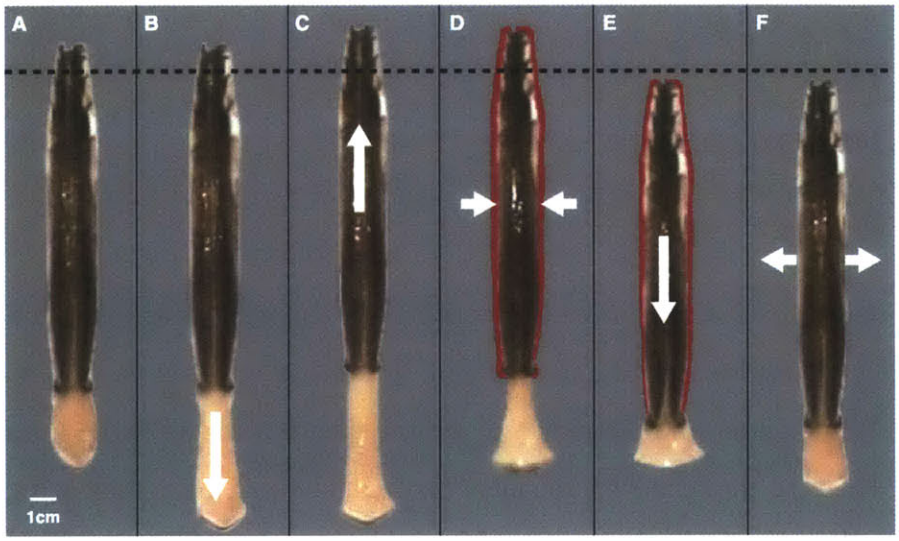

Figure 1-1: ENSIS BURROWING CYCLE. Dotted line denotes a depth datum. White arrows indicate valve and foot movements. Red silhouette denotes valve geometry in expanded state, before contraction. A) Ensis at initiation of digging cycle. B) Extension of foot. C) Valve uplift. D) Valve contraction, which pushes blood into the foot, expanding it to serve as a terminal anchor. E) Retraction of foot and downwards pull on the valves. F) Valve expansion, reset for next digging cycle. Figure adapted from [6].

An E. *directus* based anchor would be much more efficient than current anchoring technologies. The anchoring force it can achieve per energy required to insert it is greater by more than an order of magnitude compared to currently used systems [7]. Lower energy use is beneficial to any system, but is especially advantageous for energy-limited systems such as AUVs, which run on batteries and have limited capacity.

When burrowing, E. *directus* first pushes its body upward and then quickly contracts its shell (Figs. 1-1 C, D). This rapid contraction creates a region of fluidized soil around the animal's shell. This zone is created by fluid being drawn into the region around the animal. An increased fluid to particle ratio (void fraction) creates a local fluidized zone. Since the area around the clam behaves more like a viscous liquid than a particulate solid, moving downward through this region is just like moving through any other Newtonian fluid. This means there is a constant drag force with depth; in contrast, a blunt object moving through static soil encounters linearly increasing force with depth [8].

1.3 Past Work - RoboClam 1

1.3.1 Experimental Setup

RoboClam 1 is a robot that was developed to test this method of burrowing and discover the ideal performance parameters (Fig. 1-2). It consisted of an end effector that moved like and was sized similarly to a razor clam. One pneumatic piston drove the end effector up and down, and a second piston caused the end effector to expand and contract. The end effector was 7.6 cm (3 inches) long, and 1.5 cm (0.6 inches) in cross section, expanding 0.6 cm (0.25 inches) when it was in the open state (Fig. 1-3). RoboClam could vary time scales of motion, forces, and pressures associated with digging to define how to burrow most efficiently [9].

Laboratory testing with RoboClam helped define the parameter space associated with burrowing. This burrowing was done in a 363 L (96 gallon) drum filled with 1 mm diameter glass beads [11]. This glass bead media was used since it is a "weaker" soil than sand (with a lower friction angle), meaning burrowing could be performed in lab, where an infinite bed of soil is not available. To reset the soil after each test, water was pumped upward through the glass bead media, creating a fluidized bed. This was done after each test, and the drum was vibrated to resettle the beads to a more packed state. This procedure removed the disturbed region that was left in the beads

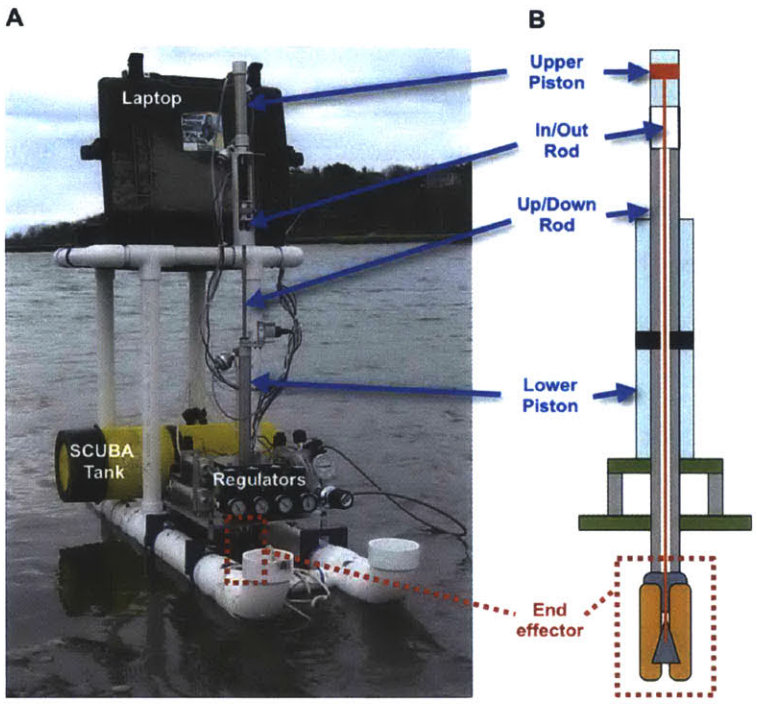

Figure 1-2: ROBOCLAM 1. This figure shows the first generation RoboClam device. A) The RoboClam setup being tested in the ocean. B) The stacked piston design of the RoboClam. The first generation RoboClam was air powered and consisted of scuba tanks with pneumatic regulators to bring the air to operating pressure for RoboClam. The upper piston moved the end effector in and out. The lower piston moved the end effector up and down through the soil. Figure adapted from [10].

after each test, resetting the media to the same condition to ensure repeatability.

1.3.2 University of Maryland PIV Testing

Particle Image Velocimetry (PIV) tests were performed at the University of Maryland, probing different time scales for contraction of the RoboClam end effector. The experimental setup consisted of an index of refraction matched particle fluid mixture in a clear acrylic box, a high speed camera, and two lasers which make a laser sheet. The index of refraction matched mixture was optically clear, meaning the camera could see through the mixture, as opposed to only seeing particles at the wall. A fluorescent dye was added, which was colored when illuminated with a laser. The laser sheet shined on the box containing the bead particle mixture, illuminating a plane in the center of the box. Particle motions in the illuminated plane were visualized by

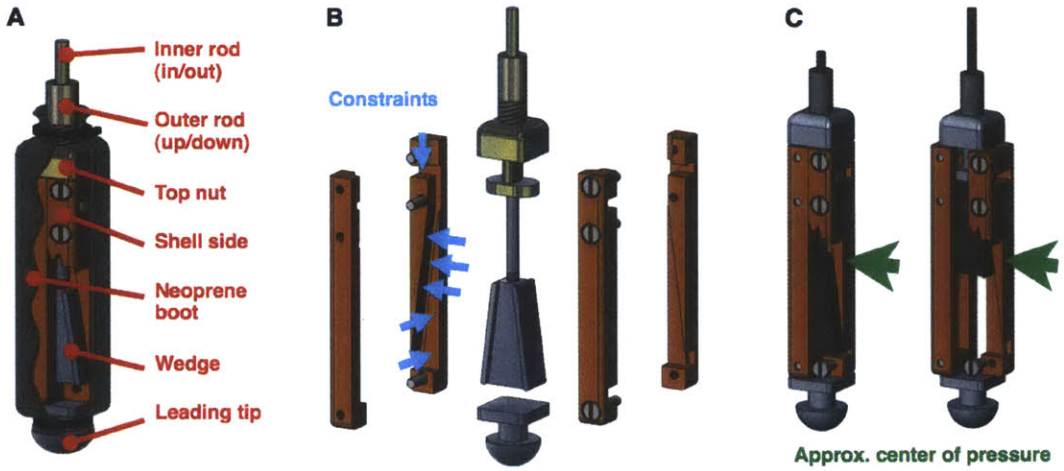

Figure 1-3: END EFFECTOR OF ROBOCLAM 1. This end effector was sealed with a flexible rubber boot to keep sand and debris out of the device. It moved in a single degree of freedom, driven by the inner rod. A) shows the full assembly including the outer boot which seals the device. It is cut away to show the interior. B) shows the constraints on the device. It is exactly constrained to move in one degree of freedom. C) depicts the range of motion of the wedge and where the center of pressure acts on the outer surface. The center of pressure always acts through the wedge so the mechanism will not jam. Figure adapted from [10].

the high speed camera.

Four series of tests were performed in this experiment in order to develop a 3D representation of soil motions around the end effector (Fig. 1-4). The first illuminated horizontal to the end effector motion showing side to side motion of the clam. The second and third setups illuminated planes 1 and 2 clam radii in front of the moving end effector. The fourth setup illuminated perpendicular to the end effector motion, showing out of plane motion of the soil particles. Time scales to contract the device from fully open to closed were varied from 0.05 seconds up to 0.35 seconds for each laser sheet location. These times span the range of possible contraction times that would work for burrowing, from faster than the max theoretical time for this fluid solid mixture and end effector size, to slower than the slowest movements that would work for burrowing [9].

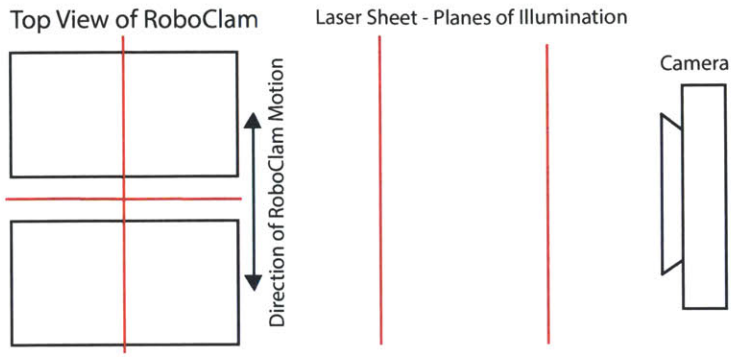

Figure 1-4: FIGURE OF UMD PIV TEST SETUP. This figure shows a top view of the testing that was done at the University of Maryland. RoboClam was put in a bed of clear glass beads and index of refraction matched fluid. A fluorescent dye was added so viewing of the illuminated planes could be done, allowing for tracking of particles in each plane. Four setups were done. Three parallel to the direction of motion, and one where the end effector was turned 90 degrees so imaging perpendicular to the motion could be performed.

1.3.3 Knowledge Gained

Testing of RoboClam 1 revealed important parameters associated with burrowing. Contracting too quickly did not give the particles time to move, whereas contracting too slowly let the particles simply slide along without ever entering a fluidized state. Re-expanding too slowly meant the particles had already settled [9].

While RoboClam 1 elucidated the fundamental behavior of localized fluidization burrowing, it was not close to being a platform for commercial applications. The actuation system was external to the end effector, located above the waterline. The device was also very small; anchoring force from a device this size would be minimal. An advanced design is needed to further understand how a device could be created for anchoring in the ocean. Understanding the design requirements and governing physics for a next generation device is important for properly sizing and designing the next generation RoboClam.

Chapter 2

Design Requirements

2.1 Performance Requirements

RoboClam 1 was designed as a research device. It consists of a small "puppet" which digs in the soil, and external actuation which is above the waterline. This device was used to understand the behavior needed to dig with fluidization burrowing.

Several lessons were learned from this device. PIV testing at the University of Maryland revealed that particles near the device were only fluidized on the sides of the RoboClam adjacent to the motion, but the sides perpendicular to motion remained mostly packed and touching the device. Partially packed soil on some sides of the device, and fluidized soil on other sides, is not ideal. Fluidization is desired on all sides of the device, since this will reduce the force required to move down as much as possible. This led to the decision to make a device with radial contraction motion so full fluidization can be achieved.

The design of the first device was such that the mechanism would never jam, as the central wedge was always at least partially located in the center of the device, where the center of pressure acts. Testing in the ocean and in lab showed that the mechanism did not jam. This characteristic is beneficial and would need to be replicated with RoboClam 2.

RoboClam 1 was pneumatically actuated. This decision was made since pneumatics have high power density and air pressure can be increased to get more force if

needed. This worked well, as scuba tanks could be brought to the ocean for testing of the device, and there was low risk of electrical shorting. Pneumatics have drawbacks for precise control, however. To control force, the pressure in the piston must be regulated. Additionally, to control velocity, the flow rate of air through the system must be controlled. Both of these systems were implemented on RoboClam 1 through the use of pressure regulators and needle valves. The infrastructure to achieve this control is complicated and takes up a lot of space. Designing a system to control an exact trajectory and force, and allow RoboClam 2 to follow this motion, was a key requirement. This would allow for changing burrowing behavior based on varying soil types, leading to further testing and optimization of ideal burrowing parameters.

2.2 Commercial Partner Requirements

Bluefin Robotics, our commercial partner on this project, is a manufacturer of commercial autonomous underwater vehicles. Bluefin Robotics seeks to use RoboClam technology to anchor their underwater vehicles to the seafloor. This is a need for several reasons. When anchored, an AUV could stay in one place without using any power, either in ocean currents or in a stream. Sea currents can cause the AUV to drift, sometimes at up to two knots. Figure 2-1 shows a depiction of how a RoboClam based AUV anchoring system would work. When a vehicle needed to stay in one place, it could deploy RoboClam from a port within the vehicle. A tether would attach RoboClam to the vehicle, and provide power to RoboClam. When the vehicle wanted to depart its fixed location, RoboClam would be commanded to burrow upwards towards the surface of the soil. The tether would be coiled back into the vehicle as it continued to move to the next location.

There are several important factors to consider when designing an anchoring system for an AUV. The design requirements for RoboClam 2 are as follows.

1. A self-contained system with an electrically powered actuator integrated as part of the device and sufficiently powerful for a variety of conditions.

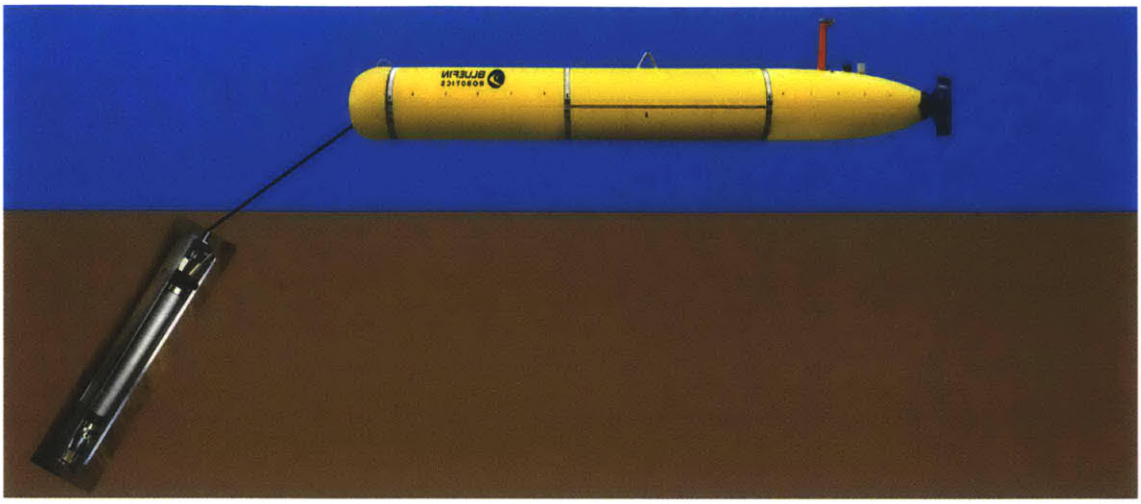

Figure 2-1: BLUEFIN 21 WITH ROBOCLAM ANCHOR. This figure shows a Bluefin 21 AUV with a RoboClam device acting as an anchor. The vehicle will have a system to deploy the anchor from its interior. The anchor will reach the seafloor and start burrowing. Upon reaching sufficient depth, the anchor will become effective and anchor the vehicle in place, preventing it from moving in currents.

2. A device sized to be carried on, and effectively anchor an AUV

3. A device that expands radially, improving digging effectiveness.

4. Move with proper motion to achieve fluidization with the lowest power possible.

RoboClam 2 must be entirely self contained and have internal actuation to allow it to be an anchor for an AUV. This device must be electrically powered since pneumatic or hydraulic systems would be difficult to implement on an AUV, where the energy is stored in batteries.

RoboClam 2 should be 5-7.6 cm (2-3 inches) in diameter to fit within existing ports in the AUV and sufficiently anchor the vehicle. It should also be short enough to fit inside of the cross section of the AUV - less than 28 cm (11 inches) long for a Bluefin 12 vehicle and 50 cm (20 inches) max for a Bluefin 21 vehicle [3]. These dimensions, as well as a physical review of the AUV, provided insight for the optimal scale of a device and helped narrow the scope of actuator technologies that work for this application.

Chapter 3

Analysis

We must understand the physics of burrowing, including soil dynamics and machine dynamics, in order to design RoboClam 2 to be capable of anchoring an AUV. The physics of the soil and how it moves leads to an understanding of soil dynamics requirements for the device, governing how the device must move to successfully fluidize the soil. From the soil dynamics, the dynamic behavior of the device is used to determine the forces needed for expansion and contraction, leading to proper actuator sizing. The device should be as efficient as possible, with the maximum amount of energy used going towards downward motion through the soil. High power motion is achievable, but overall low energy use is desirable since AUV's typically run on battery power, where the total energy available to the system is limited.

3.1 Physics of Burrowing

The physics of burrowing defines how the device moves. We must ensure that the device can easily reach a depth sufficient to keep the vehicle in place. The device must be sized such that it only needs to dig on the order of meters in the soil. This will ensure that the anchor can be quickly set and removed. The shape of the contracting body determines how the fluidized zone around the device will develop. As previously discussed, a full fluidized zone around the whole device is desired. Proper displacement of the side shells will lead to successful fluidization without

excess displacement leading to wasted energy.

3.1.1 Anchoring Force

RoboClam 2 must be large enough to sufficiently anchor an AUV in moving currents. The larger an anchor is, and deeper it is buried, the better it will hold. One tradeoff is larger anchors weight more and take more energy to transport. Deeper depth requirements mean a longer duration for anchoring and unanchoring the vehicle. For calculating the size of an anchor and depth at which it needs to be set, we can compare drag force on a Bluefin AUV with the anchoring force that can be achieved. The drag force on the vehicle is calculated using

$$F_{drag} = \frac{1}{2} C_D \rho_w A_f v_c^2, \tag{3.1}$$

where C_D is the coefficient of drag, ρ_w is the density of seawater, A_f is the frontal area of the vehicle (with 21" diameter), and v_c is current velocity. For the Bluefin 21 vehicle, $C_D = 0.25$, $\rho_w = 1029$ kg/m^3 , $A_f = 0.223$ m^2, and $v_c = 5$ knots [2.57 m/s]. This results in a drag force of 203 N for a 5 knot current. Holding force in the vertical direction for an anchor can be found using

$$F = A(c\bar{N}_c + \Delta\rho g D \bar{N}_q)(0.84 + 0.16\frac{B}{L}), \tag{3.2}$$

which is empirically derived [12], where F is anchoring force, A is the projected area of the anchor normal to the direction of tension, c is the cohesive strength of the soil, N_c is a cohesive fitting factor, $\Delta\rho$ is the difference in density between the water and soil, g is the gravitational constant, D is the anchor depth in soil, N_q is a buoyancy fitting factor, and $\frac{B}{L}$ is the fluke aspect ratio. Assuming granular, non-cohesive soils and $(0.84 + 0.16\ \frac{B}{L}) \approx 1$ for most fluke shapes yields

$$F_{anchor} \approx \bar{N}_q \Delta\rho g A D. \tag{3.3}$$

Using a least square fit for existing anchoring technologies, we get a buoyancy

fitting factor ($\bar{N}_q$) of 6.2 (which would correspond to a 45° line between the anchor and AUV) [10]. Setting F_{anchor} equal to the required F_{drag}, a device 5.6 cm (2.2 inches) in diameter, where $\Delta\rho = 493$ kg/m^3 , $g = 9.81$ m/s^2 , $A = 0.002$ m^2 results in a required anchoring depth of 2.75 m for 5 knot currents. As higher currents are typically not encountered in the vehicle's operating conditions, this is an upper limit for the depth required. For slower current, the anchor could be set closer to the surface. A device with greater area (for example by deploying flukes) would not have to go as deep to achieve the same anchoring force.

3.1.2 Fluidized Zone Shape

Achieving uniform fluidization around the entire RoboClam is desirable since this results in the most significant drag reduction [13]. RoboClam 1 is rectangular in cross-section and moves in a single degree of freedom when it expands (Fig. 3-1 top). While this was sufficient for testing, visualization with particle image velocimetry (PIV) revealed that fluidization was only occurring on the sides of the device that were moving away from the soil. Razor clams are oval-shaped and fluidization can occur around almost the entire outer surface, reducing the force needed to burrow (Fig. 3-1 middle). As such, a radially expanding device was selected as the best solution to achieve fluidization on the entire outer surface (Fig. 3-1 bottom).

3.1.3 Displacement Required for Sufficient Fluidization

In order to properly size the RoboClam 2 displacement, an analysis of the fluidized volume around the device was performed. This ensures that the shell displacement brings the region around the device to a state beyond incipient fluidization (when the particles just lose contact with each other). In order to know how much the device must contract, it is important to determine how large an area becomes fluidized upon contraction.

Two important soil properties must be measured to determine the radius of the fluidized zone. The first is the coefficient of lateral earth pressure

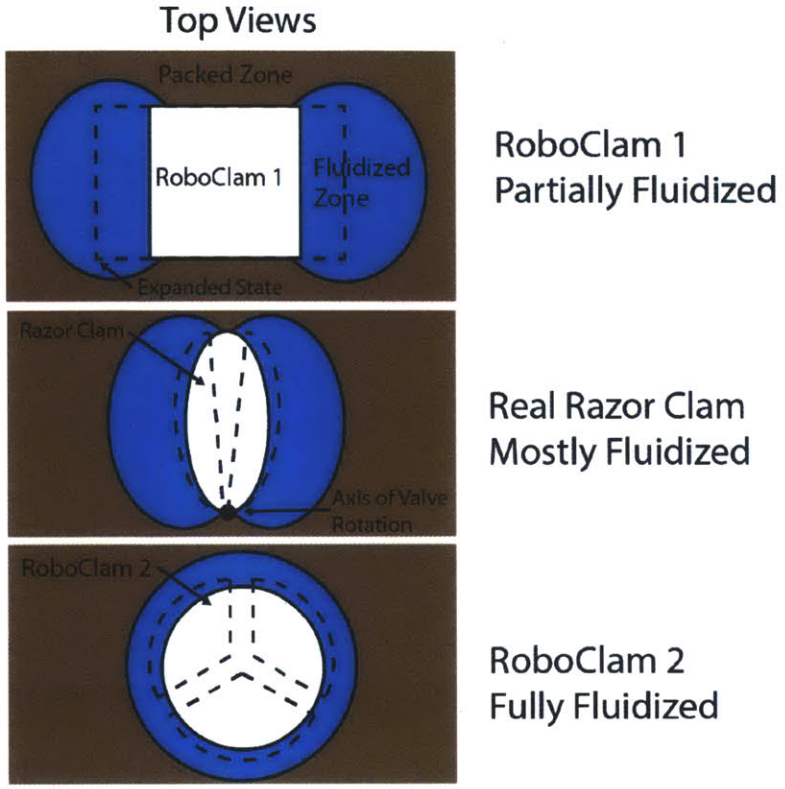

Figure 3-1: FLUIDIZED ZONE CROSS-SECTION. This figure shows a top view of RoboClam 1, a real razor clam, and the RoboClam 2 design (not to scale). The RoboClam 1 moves in a single direction. Zones to the sides of the direction of motion fluidize, but areas where contraction does not occur do not fluidize. The geometry of razor clams allows them to fluidize a much larger amount of the area around their shell. A hinge on one side of the shell allows it to expand and contract. RoboClam 2 will have full fluidization since it contracts radially. It consists of three shell pieces which move radially outward driven by a wedge.

$$K_0 = \frac{\sigma'_{h0}}{\sigma'_{v0}}, \tag{3.4}$$

where σ'_{v0} and σ'_{h0} are the vertical and horizontal effective stresses in the soil at undisturbed equilibrium. The second property is the coefficient of active factor

$$K_a = \frac{1 - sin(\phi)}{1 + sin(\phi)}, \tag{3.5}$$

where ϕ is the friction angle of the soil (the angle at which soil will support itself in a pile, without sliding to the side). Using these two parameters, we can calculate the radius of failure R_f [9].

$$\frac{R_f}{R_0} \approx \left(\frac{2}{1 - \frac{K_a}{K_0}} \right)^{\frac{1}{2}}, \tag{3.6}$$

where R_0 is the expanded radius of the device, and R_f predicts the boundary of the fluidized zone. Using a friction angle of 25° for glass beads, and the dimensions of the RoboClam 2 (diameter of 5.6 cm or 2.2 in), R_f = 5.1 cm (2.02 inches). In this failure volume around the device, we need a change in volume of 100 cm^3 (6.1 in^3) to reach a void fraction (ratio of water to total volume) of at least 41% [14]. This value corresponds to when incipient fluidization will occur for round particles. To achieve this void fraction, the displacement of each side shell radially must be at least 0.14 cm (0.056 inches). This is calculated by using conservation of volume, where the volume of particles within the failure region remains the same, but the volume of water increases to fill in the decreased device volume.

Since this is a very small contraction, we designed RoboClam 2 to have a larger contraction than this (0.64 cm or 0.25 in radially) so we can study what happens with very large volume changes. This allows for two types of studies. The first is determining what happens with different amounts of contraction. Since we use an electric actuator, we can control the displacement precisely to determine what the benefits are of different contraction amounts. Second, since the device is capable of much larger contraction than needed, we can also run the device in two configurations, one where it is contracting small amounts from its expanded state, and one where it is contracting small amounts from an almost closed state. This allows for testing of slightly different "diameter" devices which will also be beneficial to determine how accurate the scaling laws for different device sizes are in a laboratory setting.

3.2 Soil Dynamics of RoboClam

Soil dynamics govern how quickly RoboClam must move. Moving the side shells at the proper velocity is important for successfully creating fluidization. Moving too quickly will not give the particles and water time to move and will use more power

than necessary. Moving too slowly will not successfully create the fluidized zone, as the particles will just slide and settle into the void. Additionally, the depth the RoboClam moves down each contraction cycle will govern how quickly the robot can dig overall. This per cycle depth is based on the weight of the device, or how hard a two segment device could push down (see section 6.1.1).

3.2.1 Minimum Contraction Time for Soil Particles

The work in this section was previously presented in the Journal of Experimental Biology [6]. Previous testing of RoboClam 1 suggests there is a minimum time for contraction, as moving faster results in unsuccessful tests. Modeling this time is important to understand how fast a larger device should expand and contract. The minimum time for contraction that allows the particles time to move into a fluidized zone can be found based on Stokes drag [15]. This is because the Reynolds number of the fluid flowing radially inward as RoboClam contracts is relatively low [14]. The drag on the particles causes them to accelerate and move inward to the fluidized zone. Time is needed for these particles to accelerate, as moving too quickly does not give the particles time to move and the fluidized zone cannot be created. The timescale for a particle to accelerate to the velocity which the shells are moving due to Stokes drag and conservation of momentum is

$$m_p \frac{dv_p}{dt} = 6\pi\mu d_p(v_v - v_p) \rightarrow t_{min\_particles} = \frac{d_p^2 \rho_p}{36\mu}, \tag{3.7}$$

where m_p is the mass of the particle, v_p is the particle velocity, d_p is the diameter of the particle, ρ_p is the density of the particle, v_v is the velocity of a contracting valve, μ is viscosity of the pore fluid, and $t_{min\_particles}$ is the time constant of the differential equitation governing velocity change in Stokes flow [11].

Using this formula for RoboClam 1 with 1 mm glass beads in water gives $t_{min\_particles}$ = 0.075 s.

3.2.2 Minimum Contraction Time for the Pore Fluid

A second metric of interest is how quickly the fluid can move. Moving too quickly will result in cavitation of the fluid near the contracting shell surface. To determine the velocity, a small control volume (CV) of fluid near the wall of the contracting device is considered (Fig. 3-2). In the limit, when contracting, the inside face of the CV has no pressure acting on it, and the outside has hydrostatic pressure. We can relate this pressure to the force for acceleration.

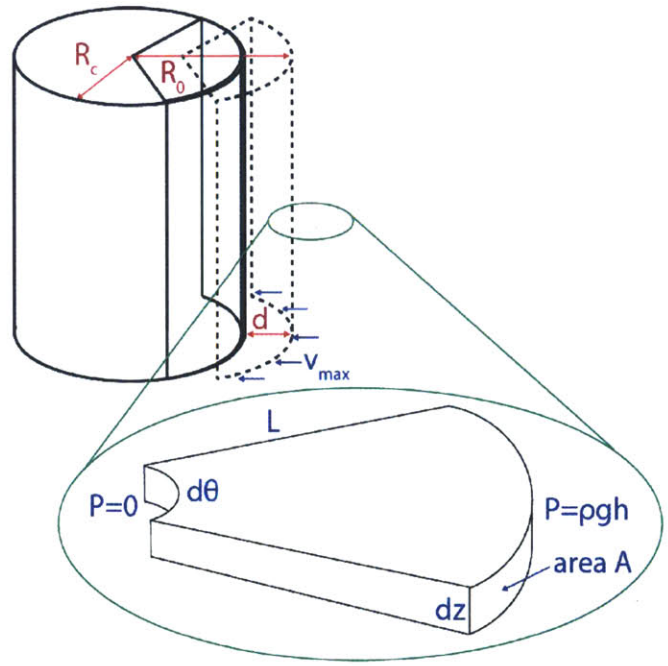

Figure 3-2: FLUID CONTROL VOLUME. This figure shows a small wedge shaped control volume of fluid at the wall of RoboClam as it is contracting. A force balance can be used on this CV to determine the maximum velocity at which it can be accelerated. This is used to determine the maximum speed at which the RoboClam should move.

$$F = PA = ma, \tag{3.8}$$

where P is the pressure acting on the outside surface, A is the area of the outside surface, m is the mass of the fluid volume, and a is its acceleration,. For a very small $d\theta$ this shape can be approximated as a right triangle. This simplifies the volume of this shape to $V = \frac{1}{2}L^2 d\theta dz$. The area over which hydrostatic pressure (ρgh) is acting

is equal to $Ld\theta dz$. Evaluating we get

$$Ld\theta dz\rho gh = \frac{1}{2}L^2 d\theta dz\rho a. \tag{3.9}$$

Canceling terms and rearranging leaves

$$a = \frac{2gh}{L}. \tag{3.10}$$

We can approximate $L \approx R_c$ since R_c is a characteristic length of the robot in the direction of interest. Integrating twice and canceling the constants of integration leaves

$$d \approx \frac{gh}{R_c}t^2 \rightarrow t_{min\_fluid} = \sqrt{\frac{dR_c}{gh}}. \tag{3.11}$$

This means that the time for contraction scales with the square root of RoboClam 2 displacement and its radius, and 1/square root of how deep it is. This means that bigger devices must move slower, taking a longer time to contract, and the deeper the device is, the faster it can move. For a device the size of RoboClam 1 at a depth of 1 m, this yields $t_{min\_fluid} = 0.087$ s. As can be seen in Fig. 3-3, the green dots clustered around the times calculated with both this and the previous analysis are successful tests. Moving much faster than this tends to result in tests that are not successful.

3.2.3 Vertical displacement through soil

For RoboClam 2 to move downward, it must push through the soil and be able to accelerate through the water. It was determined that soil, as opposed to water, will be the limiting factor for the downwards progression. When RoboClam contracts, a fluidized zone is formed at the sides of the device, radially outward from the direction of contraction. Fluidization at the leading tip of the device does not occur, however. Since the vertical stress is removed from above this soil region when fluidization occurs on the sides, the soil can be treated as static soil at zero depth (the stress state found

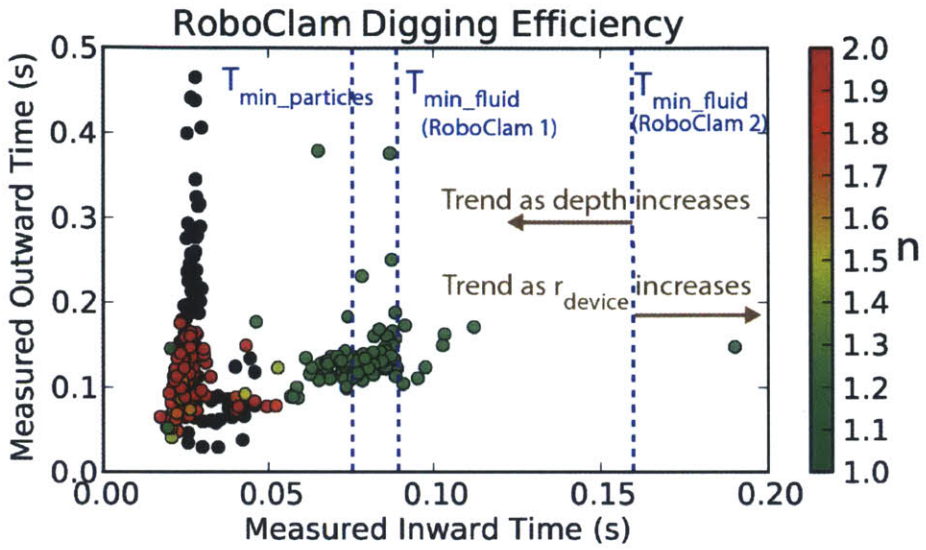

Figure 3-3: IN LAB BURROWING TESTS. This figure shows lab tests of RoboClam 1 burrowing. The color bar indicates the power law relationship n between energy and depth. Green dots (n=1) signify successful tests where fluidization occurred, red (n=2) signifies unsuccessful tests with no fluidization, and black is when the robot dug less than one body length deep [9]. The analytical $t_{min\_particles}$ (0.075 s) and t_{min_fluid} (0.086 s) are labeled on the graph. Successful tests occurred for times approximately equal to the minimum time shown by the cluster of green data points around the minimum times for the fluid and particles, but trials significantly below the minimum time were often unsuccessful (black or red dots). Notice that for larger devices, the t_{min_fluid} increases (1.68 seconds for a device the size of the RoboClam 2 at 1 meter depth). As the device burrows deeper, t_{min_fluid} decreases meaning that deeper burrowing is likely to require quicker motions.

in soil at the surface).

Determining the vertical displacement per cycle for RoboClam cannot be done analytically, but past data can be used to predict the vertical progress of RoboClam 2. Cone penotrometer tests involve pushing a cone of a known cross section into the soil and measuring the force during the process [16]. For the development of RoboClam 1, similar tests were performed with a razor clam attached to a steel rod (clamcicle). These tests were performed in the razor clam habitat in the mud flats in Gloucester, MA. Many tests were performed for a variety of depths up to 30 cm. Fitting a line to these data can be used to find the force versus depth relationship for pushing into static soil.

The clamcicle had a cross sectional area of 3.23 cm^2 (0.5 in^2). RoboClam 2 has a cross sectional area approximately 8 times larger when it is contracted. We can scale

the force required to reach a certain depth by this difference in frontal area. This will give the force required to reach the same depth for RoboClam 2. For the clamcicle, 10 N of force was required to penetrate 1 cm into the soil. Thus, approximately 80 N of force should be required for RoboClam 2 to reach a depth of 1 cm each contraction cycle. Thus RoboClam 2 must have a wet weight (mass - buoyancy force) of 8 kg to reach this 1 cm / cycle goal. Mass can be added to the front end of the device to help with the burrowing process.

3.3 RoboClam Machine Dynamics

The dynamics of the system are important for sizing an actuator for RoboClam. Understanding the maximum force needed for contraction and expansion during the burrowing process will govern the power requirements for the actuator.

3.3.1 Force for Re-Expansion in Static Soil

Properly sizing the actuator for the RoboClam device was an important part of this design. Since it is easier to move through fluidized soil than packed soil, it was determined that the maximum force that needs to be achieved is when the RoboClam is in a bed of soil, expanding from a contracted state, and the particles around the device are settled.

Mohr's circle [17] can be used to represent the stress state in the soil for passive failure (failure resulting from an increase in horizontal stress) for the soil in a settled state [18] (Fig. 3-4). The force the actuator can achieve in the radial direction multiplied by the shell projected area are used to find horizontal max stress. This is then used to determine the depth RoboClam can be buried and still passively fail the soil.

The maximum force with the current design that can be achieved in the radial direction is 278 N (the mechanism that achieves this radial force is presented in section 4.3.1). Dividing this by the projected area of RoboClam (0.018 m^2) gives a horizontal stress of 15444 Pa. We can solve Mohr's circle with Eq. 3.12 to find the vertical stress corresponding with this horizontal stress,

$$K_p = \frac{\sigma'_{push,r}}{\sigma'_{v0}} = \frac{1 + sin(\phi)}{1 - sin(\phi)}. \tag{3.12}$$

We can divide this value (6267 Pa) by gravity and the effective density of the fluid particle mixture at a settled state density (1980 kg/m^3, for a fluid, glass bead mixture with a 38% packing fraction). This yields a depth that the RoboClam can burrow of 0.323 meters, which is approximately one body length. While this depth is sufficient for current testing, greater radial force is desired for future iterations to allow RoboClam to burrow deeper. Section 4.3.2 discusses how this depth could be increased by increasing radial force for the device.

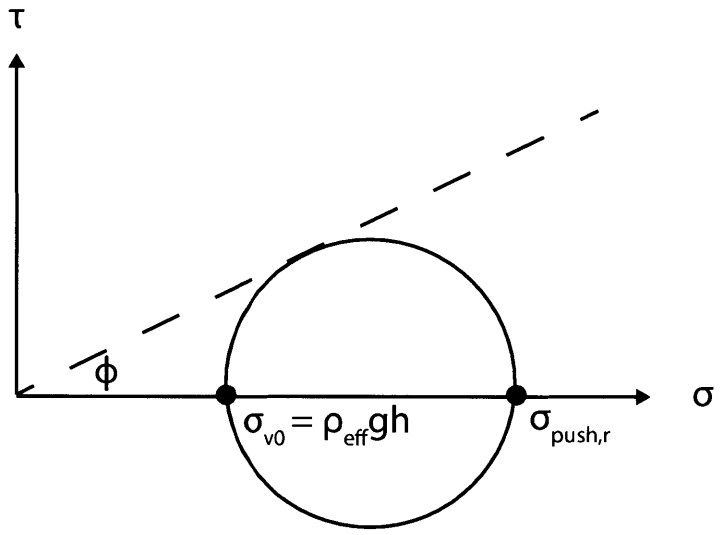

Figure 3-4: MOHRS CIRCLE FOR PASSIVE FAILURE. This figure depicts the soil state for passive failure. The depth at which the anchor is set determines how much stress is needed to fail the soil. τ is shear stress, σ is normal stress, ϕ is the friction angle (25° for this media), σ_{v0} is the vertical stress, and $\sigma_{push,r}$ is the horizontal stress.

3.3.2 Pumping Power - Max Contraction Force

An understanding of the dominate power needs for the system is important for designing RoboClam devices of different sizes. While RoboClam 2 uses one method for achieving radial motion, other methods could achieve the same motion with different design characteristics (such as lower mass and inertia or a higher force transmis-

sion ratio). Understanding the behavior of the fluid within the device is important for future designs, as the fluid is more difficult to accurately characterize than the mechanism dynamics, and can contribute significantly to device performance.

In order to calculate the power needed to pump fluid out of RoboClam through the fluid outlets, we consider the RoboClam as a annular cylinder control volume with a smaller outlet area than the cross sectional area of the annular cylinder (Fig. 3-5). This cylinder collapses as the device contracts, with the diameter of the annulus and the outlet area remaining constant. Fluid only leaves the top of the contracting cylinder, but cannot pass through the walls or through the bottom of the device.

For this problem we will consider an annular cylindrical control volume $V(z,t)$ that contracts as the device moves. This control volume ranges from the bottom of the device up to position z so the fluid velocity and corresponding internal pressure can be found at any position z.

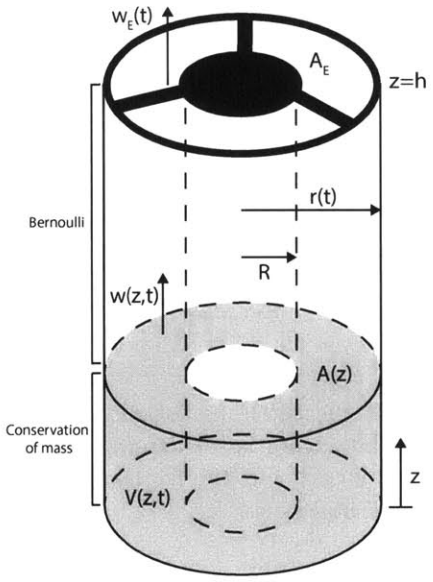

Figure 3-5: ROBOCLAM CONTRACTING. This figure shows the control volume used to find the internal pressure of water as the device is contracting. Conservation of mass was used in the control volume, and unsteady Bernoulli was used from the top of the CV to the exit of the device. Position z defines the top of the control volume, and the bottom of the streamline for unsteady Bernoulli. This position is varied from the bottom to the top of the device so the pressure can be found at any location, z

We can perform a conservation of mass analysis on the control volume. This equation

takes the form

$$\frac{d}{dt}\int_{CV}\rho dv + \int_{CS}\rho(\vec{U}-\vec{U_c})\cdot\vec{n}dA = 0. \tag{3.13}$$

The first term describes the rate of change of mass within the control volume, and the second term describes mass flow through the control surfaces.

The fluid density is ρ, $\vec{U}$ is the fluid velocity, $\vec{U_c}$ is the control surface velocity, and $\vec{n}$ is the outward facing normal.

For this case, Eq. 3.13 simplifies to

$$\frac{\partial V(z,t)}{\partial t} + w(z,t)A(z) = 0, \tag{3.14}$$

where $V(z,t)$ is the volume of the CV and $w(z,t)$ is $\vec{U}\cdot\vec{n}$, or velocity - in this case we assume one dimensional flow due to the long aspect ratio of the device. $A(z)$ is the cross sectional area of the annular cylinder.

We can rearrange to solve for the upward fluid velocity $w(z,t)$.

$$w(z,t) = \frac{-1}{A(z)}\frac{\partial V(z,t)}{\partial t}. \tag{3.15}$$

Substituting in the cross sectional area and volume for the annular cylinder yields

$$w(z,t) = \frac{-1}{\pi(r(t)^2 - R^2)}2\pi r(t)z\frac{dr(t)}{dt}. \tag{3.16}$$

To account for the change in area at the outlet, we substitute in the outlet area A_E at $z = h$

$$w_E(t) = w(z=h,t) = \frac{-1}{A_E}2\pi r(t)h\frac{dr(t)}{dt}, \tag{3.17}$$

where $w_E(t)$ is the fluid velocity through the outlet.

To determine pressure throughout the device, we must apply conservation of momentum. Since we assume it is one dimensional flow, we can accomplish this by using Bernoulli's Equation for unsteady flow between the exit surface of the control volume at z, and the outlet of the device at h [19].

$$P_E + \frac{1}{2}\rho w_E^2 + P_{loss} = P(z) + \frac{1}{2}\rho w(z,t)^2 + \rho \int_z^h \frac{dw(z^*,t)}{dt} dz^*. \tag{3.18}$$

where P_E is the pressure at the outlet, P_{loss} is the pressure drop over the outlet, $w(z,t)$ is the velocity in the device, w_E is the exit velocity, $P(z)$ is the pressure at any point in the device, and z^* is a dummy variable since we integrate with z as a limit.

We can solve this for the pressure at any location z

$$P(z) = P_E + P_{loss} + \frac{1}{2}\rho(w_E^2(t) - w(z,t)^2) - \rho \int_z^h \frac{dw(z^*,t)}{dt} dz^*. \tag{3.19}$$

Thus, the equation for the force acting on the side shells is

$$F(t) = \int_0^h P(z) 2\pi r(t) dh. \tag{3.20}$$

We will see how this model can be used in Chapter 5, when we substitute position data into this model to determine the force on the side shells, using this to determine power needed.

Chapter 4

RoboClam 2 Design

RoboClam 2 consists of an internally located, electric linear actuator, two wedges, one on each end of the device, and three shells which move radially in and out. Actuation of the linear actuator causes the wedges to slide against features on the shell resulting in expansion of the device. Figure 4-1 shows an end view of RoboClam 2. Figure 4-2 shows an exploded view of the whole device. Figure 4-3 shows the full device in its assembled form.

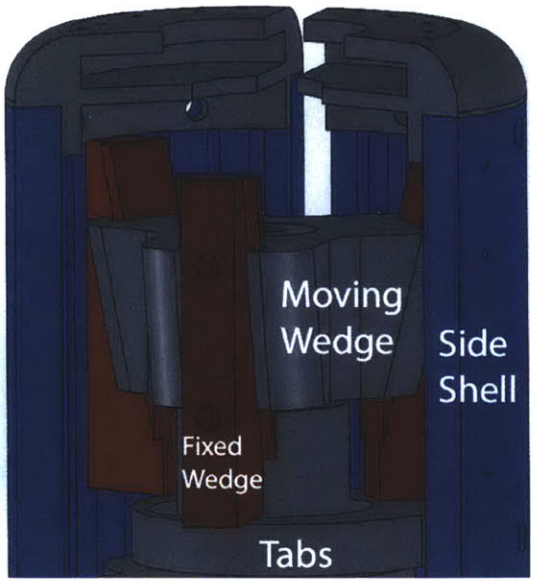

Figure 4-1: ROBOCLAM WEDGE MOTION DESIGN. This image shows the motion scheme of RoboClam 2. A central moving wedge is connected to the actuator. The fixed wedges are attached to the side shells and move radially outward. Tabs constrain the side shells to only move radially and not lengthwise with the actuator.

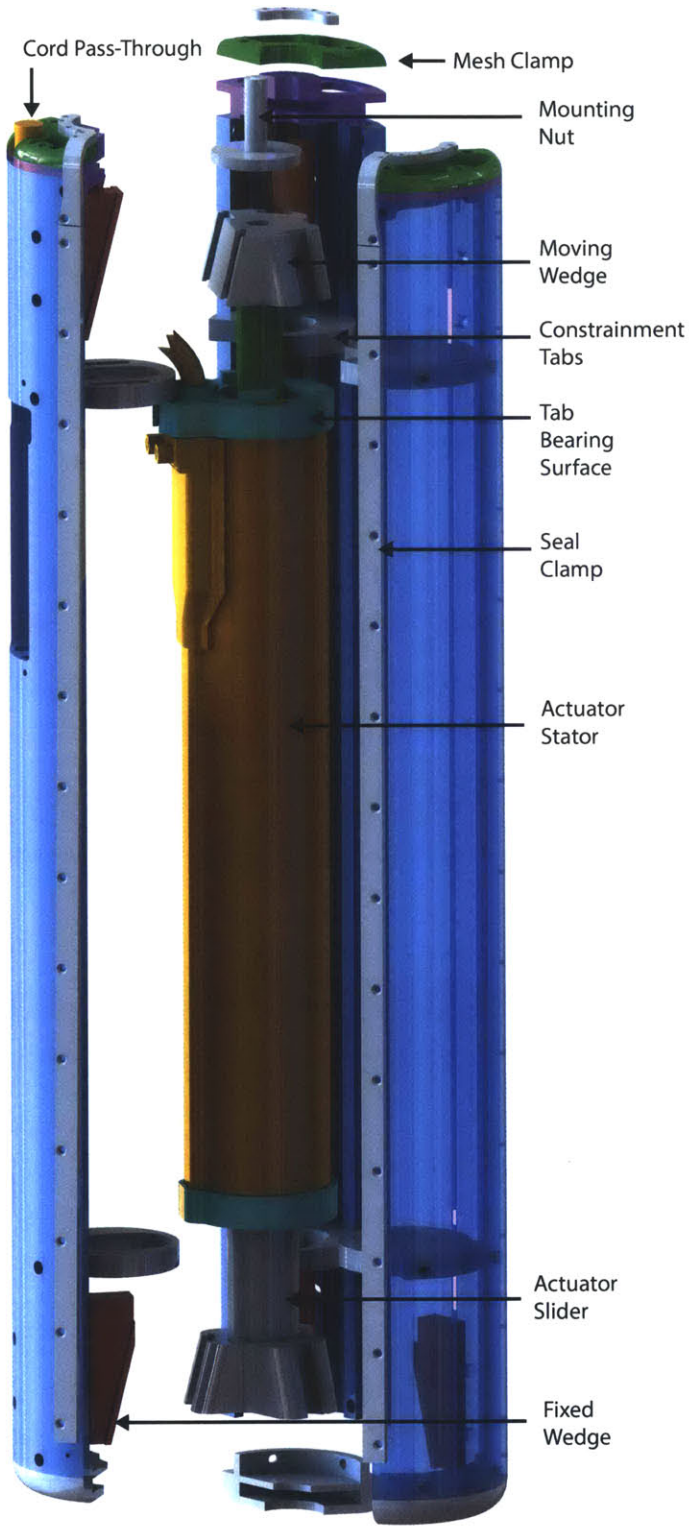

Figure 4-2: ROBOCLAM 2 EXPLODED VIEW. This figure shows an exploded view of RoboClam 2. The right side shell is rendered transparent so parts can be seen on the back side.

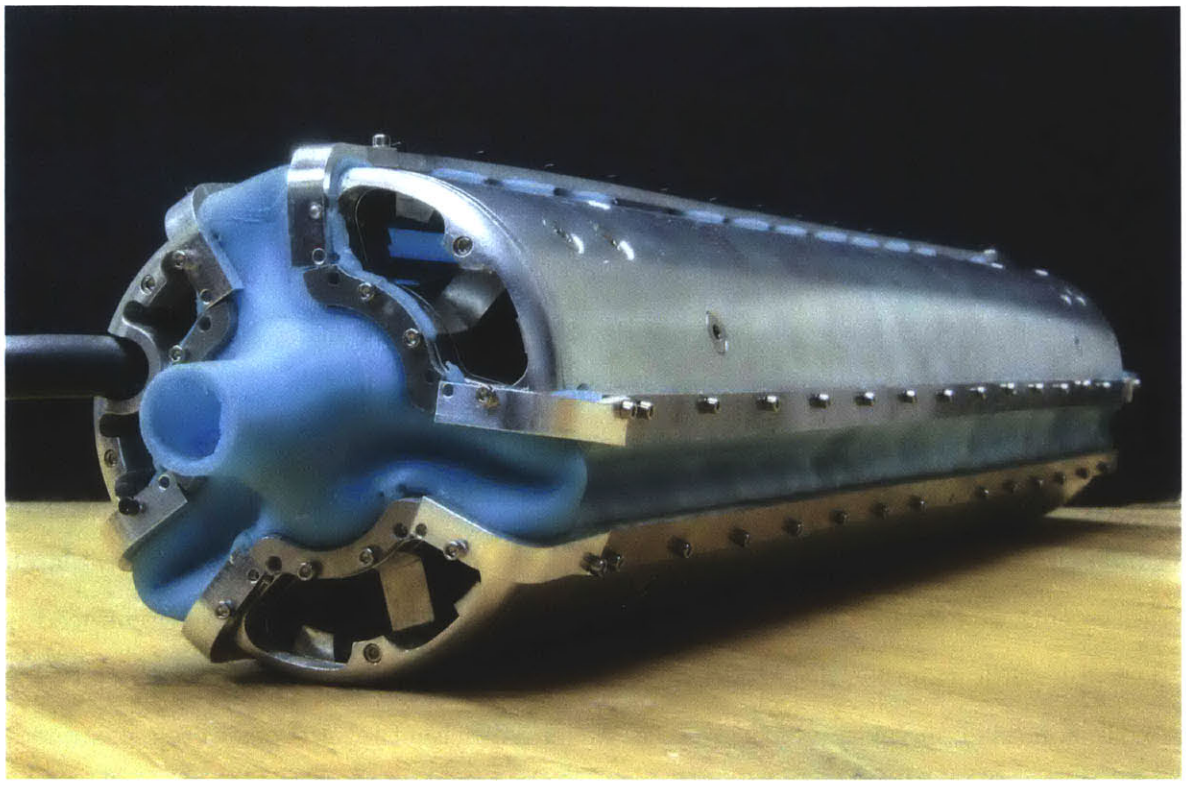

Figure 4-3: ROBOCLAM 2 DEVICE. This figure shows RoboClam 2 assembled. The flexible seals can be seen between each side shell. The water exit ports, which would be covered with mesh to prevent particles from entering, are at the top of the device (left side of image).

4.1 Actuation Methods

4.1.1 Actuation Schemes

Several methods were considered to achieve radial contraction motion of the RoboClam device. Using an off board actuator with a drive wire could be done. This wire could either spin, similar to a flexible Dremel tool attachment, or pull, similar to bicycle brakes. Two cables would be needed for pulling, one for expanding and one for contracting the device. A rigid wire could also be used to push and pull, eliminating the need for two cables pulling. These concepts would allow the device to be smaller in diameter, as it would not need to house the actuator.

4.1.2 Actuator types

A linear or rotary actuator inside the device could be used to achieve motion needed for contraction. With rotation, small pulleys and cables could be used to contract the device. Springs could be used to re-expand the device. Similarly, with only small amounts of rotation, linkages could be used to expand and contract the device. Shape memory alloy (SMA) wires were considered for use in actuating RoboClam. These actuators have very high power to weight, but are fairly inefficient. The wires contract 4.5 - 8% of their length, so getting sufficient displacement for actuating the device would require complex wire routing [20]. It is also difficult to control the speed at which the wires actuate, meaning they would not be as useful for creating a research device with the goal of understanding soil properties, as varying contraction speed is desirable. Additionally, SMA wires can only pull, so two sets would be necessary for expansion and contraction of the device. Several other actuator types were considered, and the pros and cons of each are summarized in Table 4.1.

Table 4.1: Summary of Actuator Types

Actuator	Pros	Cons
Pneumatic	Good in Water Fast	No Air on AUV or Ocean
Hydraulic	Good in Water High Forces	Slow Not on AUV
Electric - Rotary	Cheap Many Embodiments	Difficult Mechanism Needed Gearing Needed
Electric - Linear	AUV Battery Powered Fast Can Control Speed	Expensive
Memory Wire	Easy to Use High Power:Weight	Low Efficiency 8% Contraction Difficult to Control Speed

4.2 Actuator Selection

An electric actuator was selected for the internally actuated design [21]. Using an electric actuator is desired since it uses the same power source that is readily available

in an AUV. It can also have a very high power density and can accelerate much faster than other actuator types. The selected actuator was a convenient choice because it is a radial form factor that was easily implemented in the RoboClam 2 design. It allows for accurate position control and the ability to control velocity of motion, a benefit over pneumatic actuators. This will allow for probing the characteristic times for digging and lead to the discovery of optimal timescales, as moving slower requires less power, but moving too slowly will not create the fluidized zone. The actuator is also waterproof and corrosion resistant, allowing for testing in water.

After selecting the linear actuator, many different schemes were considered for how to convert vertical linear motion of the actuator to outward motion of the side shells. This could be accomplished with a series of linkages, pulleys and cables, or gears. Sliding contact wedges were selected for their simplicity, robustness, and since they were used successfully on RoboClam 1.

4.3 Sliding Design

A double wedge design was used for actuation of the shells. There were two benefits to this design. Having two wedges prevented the device from jamming since the center of pressure of the soil acted between these two wedges. Locating these features at the ends allowed for a smaller diameter, longer device. This was beneficial since power scales with the diameter of the device.

Stainless steel and bronze were selected for the sliding components in RoboClam 2. These materials were used in RoboClam 1 with success due to their corrosion resistance, high strength and durability, and low coefficient of sliding friction on each other when lubricated. Since there was an opportunity for the seal to break during testing, it was important to use durable materials that would hold up even when the mechanism was jammed, and filled with particles.

Upon receiving the machined parts, friction in the mechanism was found to be too high. Simply holding the device with one hand could prevent it from opening under peak actuation force. To fix this, the surfaces of the sliding contact regions were

polished smooth with 6 micron diamond polishing paste, which noticeably improved the sliding friction between the parts. To further reduce friction, waterproof grease was added to the wedges before the device was assembled.

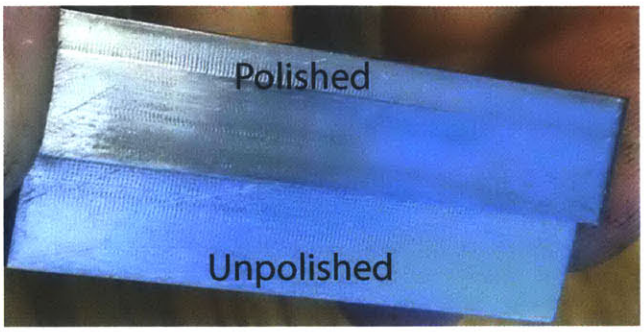

Figure 4-4: WEDGES BEFORE AND AFTER POLISHING. After polishing with diamond paste, the wedge on the top is much smoother than the wedge on the bottom, which has not been polished.

4.3.1 Friction Analysis

A free body diagram (Fig. 4-5) was used to analyze the force transmission ratio of the mechanism. We are interested in the ratio of force out when compared to force that the actuator provides (Force transmission ratio = $F_{shell}/F_{actuator}$). This will tell us how much force is available to be applied to the soil and pumping of water, and how changing parameters such as the angle of the wedges used for actuation, θ, and friction, μ, will affect the device. Achieving a high force transmission ratio is desirable, as this increases the depth RoboClam can dig, and the speed at which it can dig.

We can solve for $F_{actuator}$ in terms of other knowns, where $F_{friction} = \mu N$ with

$$F_{actuator} = 2\mu N cos(\theta) - 2N sin(\theta). \tag{4.1}$$

We can solve for F_{soil} in a similar fashion

$$F_{shell} = N cos(\theta) - \mu N sin(\theta) - \mu F_{constraint}. \tag{4.2}$$

Substituting $F_{constraint} = N sin(\theta) + \mu N cos(\theta)$ yields

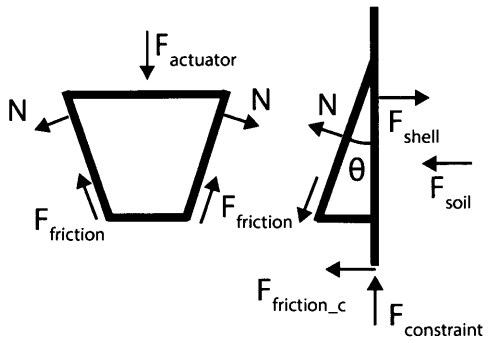

Figure 4-5: FREE BODY DIAGRAM OF ACTUATOR MECHANISM. This free body diagram shows the forces acting in the sliding mechanism of the device. The force from the actuator is split between the three side shells; only one is depicted. Variables: $F_{actuator}$ is the force the actuator can produce; θ is the angle of the wedges in the mechanism design, 14° for this device; $F_{friction}$ is the frictional force, equal to μN; N is the normal force between the sliding and fixed wedge; F_{shell} is the force the shell can exert on the soil; and F_{soil} is the force the soil exerts on the side shell. F_{shell} must exceed F_{soil} for the device to expand. $F_{constraint}$ is the force that the tabs exert on the side shells to constrain them to only radial motion. $F_{friction\_c}$ is the frictional force from this constraint.

$$F_{shell} = N[cos(\theta) - \mu sin(\theta)] - \mu N[sin(\theta) + \mu cos(\theta)]. \tag{4.3}$$

We can then find the force transmission ratio

$$\frac{F_{shell}}{F_{actuator}} = \frac{[1 - 2\mu tan(\theta) - \mu^2 cos(\theta)]}{2[\mu + tan(\theta)]}. \tag{4.4}$$

For the design parameters of this device ($\mu = 0.16$ [22] and $\theta = 14°$), we get a force transmission ratio of 1.09. This could be increased by either reducing the friction or reducing the angle, θ.

4.3.2 Mechanical Efficiency

We can find the mechanical efficiency of the mechanism based on this force transmission ratio. Since the device expands a total of twice each shell's individual deflection, the device has an effective gearing of 2:1. Thus for each inch the actuator moves, the device expands half an inch in diameter. With a force transmission ratio of 1.09, the device has a force transmission efficiency of 55% (force transmission ratio / gear ratio).

The results of the last two sections are summarized in Table 4.2. Teflon on teflon sliding surfaces could be used ($\mu = 0.04$) [23], the angle of the wedge could be reduced from 14° to 7°, or both could be done.

Table 4.2: Case Study for Wedge Design

Parameter	Current	Teflon	7° Wedge	Teflon and 7°
μ	0.16	0.04	0.16	0.04
θ	14°	14°	7°	7°
Gear Ratio	2:1	2:1	4:1	4:1
Force Trans. Ratio	1.09	1.69	1.65	3
Efficiency	55%	85%	41%	75%

For future iterations, teflon coated surfaces could be used to maintain structural characteristics of the sliding wedges while reducing friction. The wedge mechanism used in RoboClam 2 was not optimized for efficiency; rather, a geometry was chosen to fit within the packaging constraints of the device.

4.4 Seal Design

Sealing was achieved with a rubber strip, similar to a baffle, mounted along all of the expanding joints of the device. A tube-shaped rubber boot was used in previous prototypes, but high forces were needed to expand this seal. Strips along the device were flexible and folded as the device contracted. Expansion of the device caused the strips to straighten but did not put them in tension. Fig. 4-6 depicts a bench level prototype validating this sealing method.

Several different methods were considered for how to achieve proper sealing for the device (Table 4.3). The linear actuator needed to be cooled, as it generated heat as it ran. This meant that water or air needed to enter and leave the space around the actuator to bring the heat out of the device. Table 4.3 shows the process used to select the best sealing method. The vertical categories represent the possibilities for how fluid will interact with the control volume, and the horizontal categories are how the seal could be designed. "Water and vents" means water would enter and exit the device through vents at the top, where a mesh would keep particles out. The "air

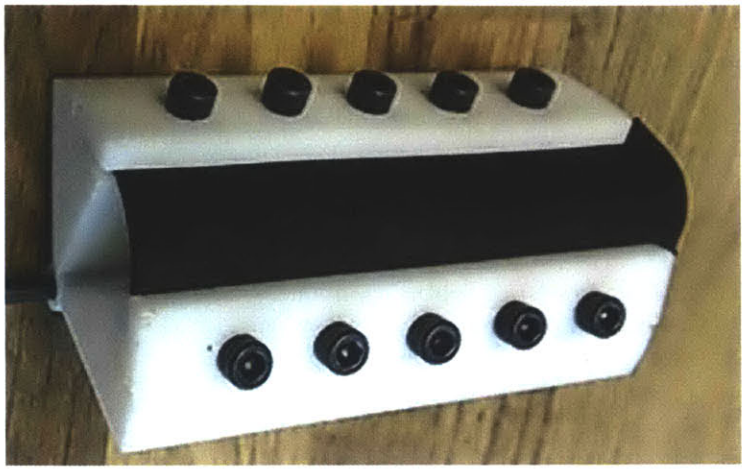

Figure 4-6: SEAL TEST MOCKUP. This 3D printed device was a test to validate the concept for the seal for the second generation RoboClam. This figure shows the prototype of the seal that was used on the edges of the RoboClam to seal out debris. The seal is not stretched when expanded, which reduces the force needed to expand the device. When RoboClam is contracted the seal folds on itself, which requires very low force.

filled" and "water filled" categories mean the device is a sealed CV, and "bladder" means the liquid will flow out of the contracting device into a bladder. The bladder is the most similar to how the razor clam acts, with blood filling the animal's foot and water shooting out of the siphons when the shells contract.

"Sealed along edges" means the shells have seals that are attached to the edges of the shells, and as they contract the seal allows for motion. "Tightly stretched" is a full "boot", similar to covering the device with a party balloon, which is stretched when the device expands. RoboClam 1 used this concept. "Loosely stretched" is a balloon-like cover, but the size is larger than the size of the device in its contracted state.

The option that was selected was "water and vents". This allowed the actuator to be cooled but did not require a large bladder. It accounted for the changing size of the device. "Sealed along edges" was selected as this was the most controlled option, and we could control what happens with the seal when the device contracts.

Table 4.3: Fluid Sealing Options

	Sealed Along Edges	Tightly Stretched	Loosely Stretched
Water and Vents	Hard to Seal Perfectly Pumping Losses Filter Needed Most Durable	Takes power to make expand	Water won't go out vents but between wall and seal
Air Filled	Air Compressed at depth Cooling not achieved Hard to prevent air escape	Air needs to go somewhere	Fixed amount of air inside
Bladder	Hard to Seal Perfectly Pumping Losses		Bladder won't fill, water just goes between wall and seal
Water filled	If sealed CV, size change will not allow water to go anywhere	Nowhere for water to go	Water fills between wall and seal

4.4.1 Seal Fabrication

Side seals were created by casting silicone sold by Smooth-On [24]. Custom molds were 3D printed (Fig. 4-7) with a cavity the shape of the desired seal. Silicone was poured into the cavity and cured to a rubber-like texture. Five total pieces were used to create the seal; one piece for each end, and one strip to go between each shell. They were glued together using silicone adhesive.

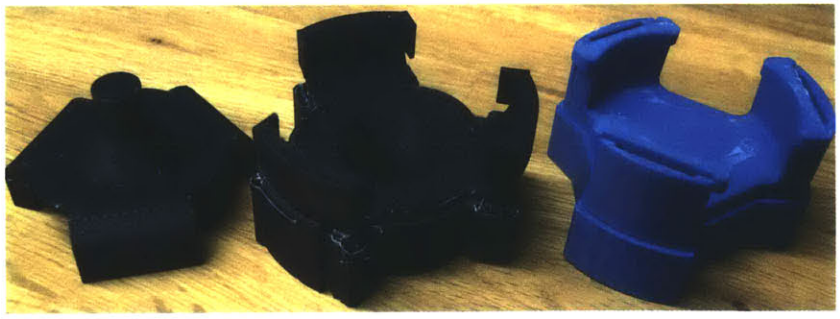

Figure 4-7: SEAL MOLDS. This figure shows the molds used to produce the seal pieces for either end of RoboClam.

4.5 Fluid Outlets

As the device expands and contracts, there is a volume change of 4.7 x 10^{-4} m^3 (28.7 in^3) which is 54% of the volume of the device in its contracted state. Numerous solutions were considered to allow the device to expand in this manner. As discussed, the device could be filled with air and the air could be pumped into a bladder at the end of the device when it contacts. This would not work effectively however, since the actuator needs to be cooled and air has a low heat capacity. Water-cooling was necessary. A bladder for water would also work, but it was decided that fluid vents at the top of the device would allow the fluid to move in and out. The size of the bladder would also have been significant when compared to the size of the device. Since water has a viscosity 50 times higher than air, the vents needed to be sized appropriately to prevent hydrolocking the device.

Figure 4-8 shows the bench-level setup that was used to determine if the desired outlet size was sufficient. A pressure drop of less than 6.9 kPa (1 psi) was measured over the mesh for the necessary fluid flow rate, thus this area was sufficient for RoboClam 2. A mesh over the vents prevents glass bead test media from entering the device, and only allows water to flow through.

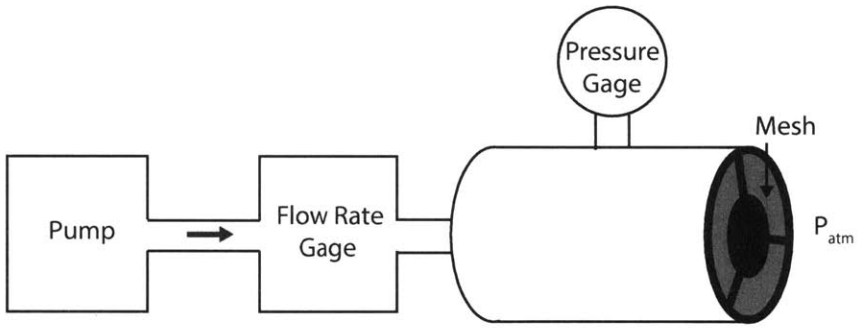

Figure 4-8: FLUID OUTLETS TEST SETUP. This figure shows the flow of water through a bench level prototype testing the restriction to fluid flow through the RoboClam. A mesh located in this test is the same area and shape as mesh located at the top of the RoboClam 2. At the necessary flow rate, the pressure drop was measured at under 6.9 kPa

Vents were added in the end rather than the sides of the device to restrict flow to only the ends. The theory generated about how the device digs is based on the fact

that rapid contraction quickly draws water inward radially towards the device. This pulls particles with and creates a fluidized zone. Vents on the side of the device would be effectively blowing water into this fluidized zone, changing the soil and mechanics of local fluidization. Future iterations of the device could use side vents for the water, which could increase fluidization and improve digging efficiency. They could also have much larger surface area, which would lower the forces required to pump the water out of the device.

4.5.1 Fluid Channels

Fluid channels (Fig. 4-9) were added in the inner surfaces of the side shells. Early design iterations of the side shells had inner curved surfaces and features for mounting the mechanism. The features prevented the flow of water upward through the device. Channels were added in the side shells to allow uninterrupted flow of water from the bottom of the device up to the top vents, preventing hydrolocking.

Instead of channels in the sides, an easier method to create a path for water flow would be creating pockets in the tabs (the features on the side shells which prevents vertical motion of the shells when the actuator moves). This would allow for simple geometry on the inner surface of the shells, and maintain the same cross-sectional area for water to flow upward through the device.

4.6 Device Dimensions

The RoboClam 2 device is 5.6 cm (2.2 inches) in diameter when fully contracted. The device expands to a max diameter of 6.9 cm (2.7 inches). It is 38.4 cm (15.1 inches) long. The radius of the stator of the actuator is 1.85 cm (0.728 inches). The device contracts at a maximum rate of 0.054 m/s. It has a dry weight of 3.6 kg, and a wet weight of 2.4 kg.

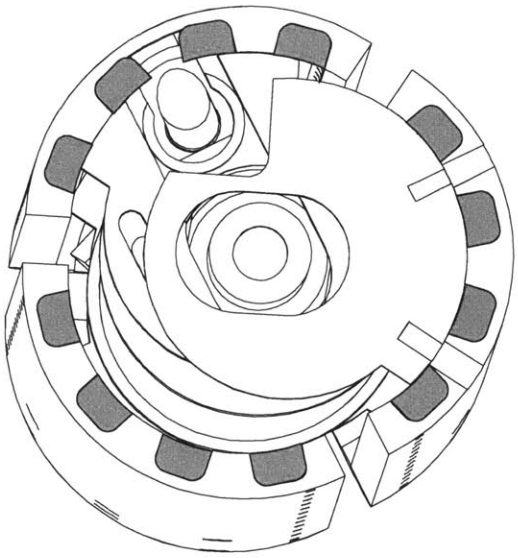

Figure 4-9: FLUID CHANNELS. Channels were added in the side shells (depicted by the gray highlighted regions) to allow for flow of water from the bottom of the device up to the mesh vents at the top.

Chapter 5

Testing

5.1 Control Method

The LinMot linear actuator used in the RoboClam device has two methods that can be used to control its motion. Since it is commonly used in commercial applications, the motor driver is equipped with the ability to program predetermined moves. A programmable logic controller can send the motor driver commands, and the actuator will perform these motions. This is typically how the drive operates, as it is capable of performing exactly the same motion hundreds or thousands of times per day.

Using the actuator for RoboClam was difficult. Since we were trying to use the actuator to characterize the soil properties, but did not have a full understanding of the forces and motion needed, the actuator required logic to perform the correct motion. The actuator could receive serial communications from a computer, and we used MATLAB to send these commands. The current draw and position of the actuator could be know in real time in this scenario. Using this information, the commanded position and force could be updated throughout the move. This was necessary because by default, the actuator would give an error message if the drive was not moving with a certain amount of current applied. This happened if the load was higher than expected by the driver software's preset load defaults. The drive also gave an error if the commanded position deviated too far from the actual position of the actuator. This occurred when the commanded motion was too fast,

with force that was too low. Even peak force was not sufficient for all desired motions; RoboClam 2 required sufficient time to pump all water out of the device as it was contracting, thus instant contraction was not achievable.

5.2 Test Results

5.2.1 Water and Air Contractions

Several different methods were considered for how to determine the dominant power needs of the system. The first was finding and comparing the effective mass of the mechanism and the water. This involved finding the acceleration of the device when contracting in air and water and using the force data obtained from current measurements during a contraction cycle. Conservation of momentum was used to find the effective mass for device and water, and effective mass for device alone. This method was abandoned since the acceleration data was very noisy, and results from this analysis did not make sense.

A second method was considered for determining the dominant power needs. Looking at the current spikes during contraction and expansion revealed high force periods during the movement of RoboClam. This could be used to see if inertia or pumping in the system was dominant. For an inertia dominated system, peaks in force (current) were expected at points of max acceleration, as it took large amounts of force to overcome the inertia of the system at rest. For a system dominated by pumping power loses, force peaks were expected during times of maximum velocity, as moving faster corresponds to pumping fluid faster. This method was abandoned, as inductance in the motor can limit how quickly the current can ramp to a maximum value. This lag made it difficult to identify when peak force was needed; higher current might have been demanded during the acceleration period, but not available until the max velocity period.

The method that was selected to determine dominant power needs was comparing the power used during motion with and without water. Determining the power needed

to move the fluid in RoboClam 2 was done experimentally. These data were compared to the analytical model for pumping fluid out of the device (Section 3.3.2). For a contraction cycle, we calculated the power needed to move the device by knowing the force and velocity of the actuator. In water, power accounted for moving the actuator (accelerating, decelerating, and overcoming friction in the device) and moving water. In air, the power was only used for moving the actuator and overcoming friction. To determine the power to move fluid, the difference between these two was found with

$$Power_{water} = Power_{actuate\_in\_water} - Power_{actuate\_in\_air}. \tag{5.1}$$

Equation 5.1 assumed the kinematics of the motion were similar, resulting in similar power to overcome inertia in each case. To achieve the same kinematics, we commanded the actuator to move with a known position profile and calculated the actual position profile and the force during the cycle.

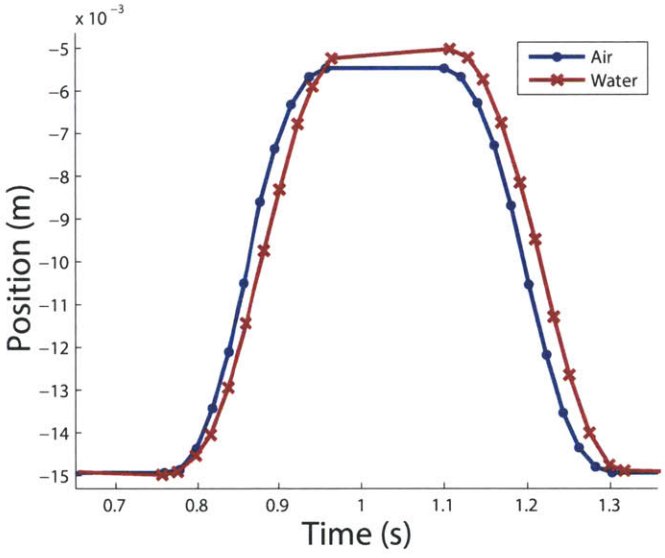

Figure 5-1: CONTRACTION IN AIR VERSUS WATER. In this plot a contraction, pause, and expansion cycle is shown for RoboClam. Contraction of 10 mm total for linear actuator motion corresponded to approximately 5 mm contraction in diameter. As can be seen by the slopes, contraction in water was slower than contraction in air. This can be accounted for due to the differences in power needs for moving with water and air. Proper tuning of the controller could further minimize these differences, but they were expected for such different contraction conditions.

Figure 5-1 shows the position versus time profiles for moving in air and water.

Both profiles are fairly similar. Due to actuator constants, the velocity when moving in air was slightly faster, though similar enough for an adequate comparison of power between the two cases.

To find power for the motion, we calculated the force during a motion cycle, achieved by multiplying the current draw by the motor constant ($17\ \frac{N}{A}$) for the LinMot linear actuator used in RoboClam 2 [21]. We found velocity by differentiating the position profile with respect to time. The product of force and velocity gave mechanical power of the device (Fig. 5-2). For a contraction and expansion motion, a large percentage of the power is used for moving the fluid. It is expected that for moving faster, an even greater percentage of the power would be used to move the fluid.

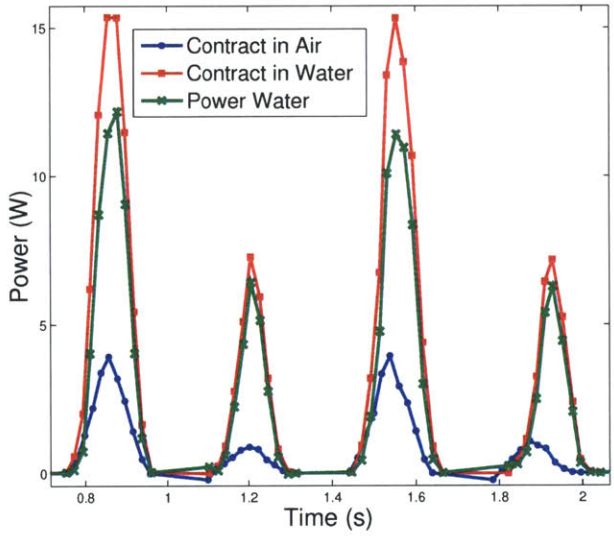

Figure 5-2: POWER USE. Power is plotted against time for two contraction-expansion cycles (contract, expand, contract, expand). This was done for two different conditions, first for the mechanism when moving in air and then for the mechanism moving in water. The power for moving the water was the difference between the two. For motion in air, differences in power between contraction and expansion can be attributed to variations in directional friction, variations in force to move the seal, and steel tabs in the device, which are attracted to the magnetic portion of the actuator.

With this analysis, we show that we can accurately identify fluid effects in the system. We now have a framework for understanding the mechanical and fluid power needs for the system, which can be used to determine power requirements for different

device sizes.

5.2.2 Comparison to Pumping Model

Validating the analytical model for pumping power was done using experimental data by investigating the motion that is achieved when RoboClam contracted when filled with water. We used the position recorded by the actuator to determine $r(t)$ and its derivatives. These were substituted into in Eq. 3.16 as $\frac{dr}{dt}$. The parameters for RoboClam 2 were outlet area $A_E = 8.59 \text{ x } 10^{-4}$ m^2, $\rho = 1027$ kg/m^3, length $h = 0.355$ m, actuator radius $R = 1.85 \text{ x } 10^{-2}$ m, and exit pressure $P_E = 0$. We substituted the result into Eq. 3.19 to calculate the pressure on the inside of the device. We then integrated over the height of the device and multiplied by the projected area to find the total force. Power was calculated from this by multiplying force and shell velocity. The power calculated analytically was then compared to the measured power for moving the water, presented in the previous section.

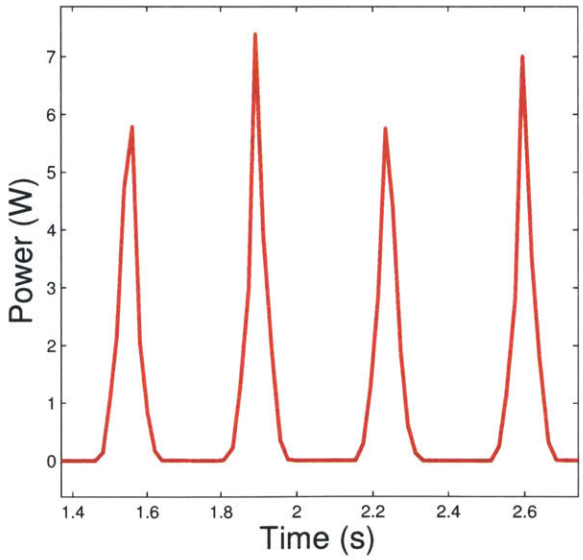

Figure 5-3: SIMULATED POWER USE. A plot of power use vs time for contraction-expansion cycles shows that when using the motion trajectory of RoboClam, the analytical model presented is an accurate representation of the power needed for contraction. This can be seen by comparing this data to the power consumption for moving water (shown in Fig. 5-2). The model underestimates the power needed since the loss coefficients used in the model were conservative for this situation.

The predicted power (Fig. 5-3) is within a factor of two from the actual power used to move the fluid during motion of RoboClam. This model is beneficial for future designs, as power predictions can be made for larger size devices, allowing for proper actuator sizing. Discrepancies in the plots are based on simplifications made when modeling the pressure drop over the complex internal features in RoboClam. Additionally, the flexible seal was folded inward and slightly reduced the cross sectional area of the device. Correction factors could be added to the model to account for complex internal geometry which will bring the predicted power value closer to the analytical result.

5.2.3 Digging Tests

Digging tests were performed in the lab using the RoboClam 1 experimental setup, consisting of a 96 gallon drum filled with 1mm soda lime glass beads. A pneumatic actuator was used to guide the robot to dig vertically and apply a force in the burrowing direction (simulating a heavier device). Vertical position was measured by locating the position of the piston, as it extended above the soil surface. During each test, RoboClam would expand and contract.

With 71.5 N of applied force, RoboClam 2 was able to reach a depth of 13.7 cm (5.4 in) before the actuator could no longer apply sufficient radial force to expand the device (Fig. 5-4). This was partially due to the control method used; the actuator would freeze when it reached this depth, no longer pushing at full force, and unable to contract and expand. Achievable depth could be increased by improving the actuator performance or selecting a more powerful actuator.

Vertical displacement per cycle was less than the predicted 1 cm per cycle except for the first few contraction cycles. This was likely due to the soil at the tip of the device not behaving exactly like the soil at the surface, as was approximated in section 3.2.3, once the device was several centimeters into the soil. Vertical displacement per cycle could be improved by increasing the distance the actuator contracts, which would increase the amount of fluidization around the device, and further relieve the stress in the soil at the tip of the device.

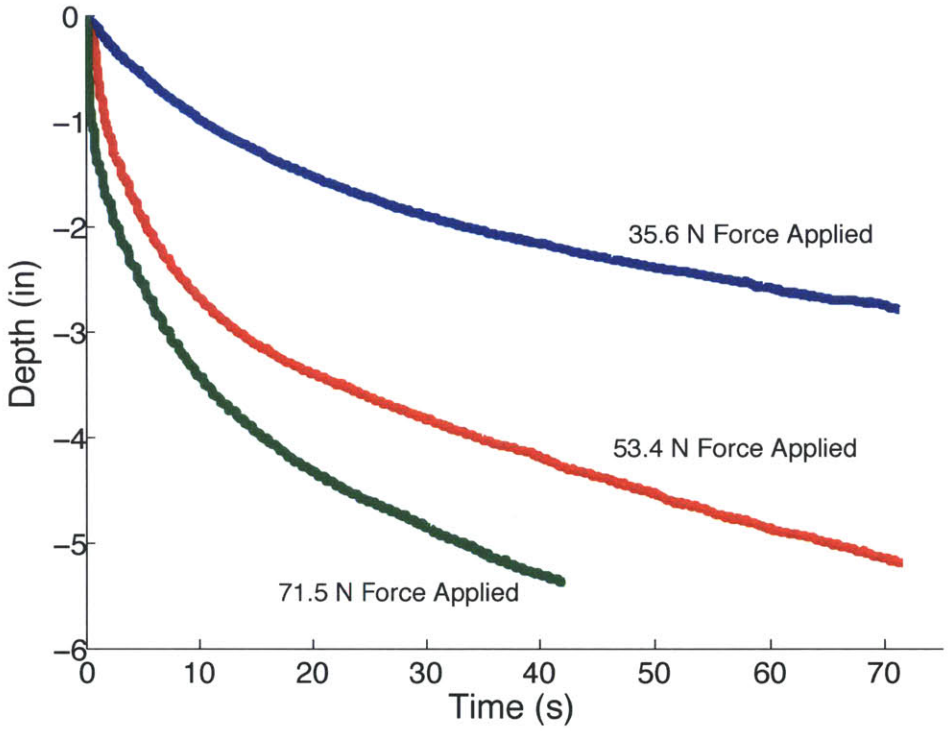

Figure 5-4: BURROWING TEST RESULTS. This plot shows the burrowing of RoboClam 2 with varying downward forces applied during the burrowing process. For each test, a pneumatic piston was used to push the robot down with varying force, and the device was commanded to contract and expand. Depth values start with zero when the RoboClam was at the soil surface. As burrowing progressed, the depth per contraction cycle decreased, as the device required greater force to fully fluidize the surrounding soil. Larger applied downward forces led to more rapid digging, as the depth per cycle that could be achieved was larger.

Chapter 6

Conclusions

6.1 Future Work

RoboClam 2 was designed as a device which will allow continued testing of parameters in the lab. It was designed based on Bluefin Robotics' requirements, and has internal actuation. To work as an anchor for their vehicles, there are several improvements that should be made. The seal that keeps grit out of the mechanism should be made more durable. Additionally, it is recommended that pushing water radially outward through the device shells should be tested. Filters in the shells would allow water to travel out of the mechanism but prevent small particles from getting in. Since the hole size in the filters would need to be smaller to operate in the ocean as compared to operating in glass beads, larger total vent area would be required. Additionally, having two devices stacked together would allow the mechanism to dig down, then dig back up when the vehicle is ready to leave (Fig. 6-1). Methods to increase the size of the device would allow it to burrow to shallower depths and still act as a sufficient anchor. To achieve higher power density in a small form factor, a hydraulic actuation system could be used in the vehicle to actuate RoboClam.

6.1.1 Two Segment Design

Currently the RoboClam can either dig under its own weight or be pushed down from the top to simulate an attached weight. While this works in the lab, for the RoboClam to be able to undig from a burrow, it would be beneficial for it to move in either direction. A two segment system can be used to achieve this motion. Fig. 6-1 shows how this could be achieved.

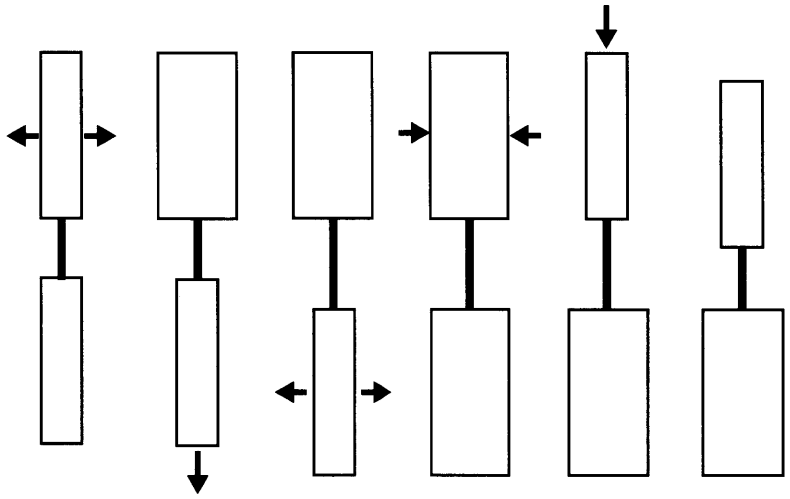

Figure 6-1: TWO SEGMENT MOTION. This figure shows the motion that could be achieved by two RoboClam modules linked together by a length change section in the center. The top segment would expand then push the bottom segment down. Then the bottom segment would expand. After this, the top segment can contract and then move down, completing one digging cycle [25].

6.1.2 Fluke Area Increase Method

With the current cross-sectional area of RoboClam 2, the anchor would have to be set about 3 meters deep to sufficiently hold a Bluefin 21 AUV. Increasing the cross-sectional area of the RoboClam could reduce this depth. It is desirable to have a small cross-sectional area when burrowing, and increase it once the device has dug to the desired depth. Fig. 6-2 shows two concepts for how this area increase could be achieved. Since anchoring force scales linearly with cross-sectional area, having deployable flukes could significantly decrease the required depth for burrowing.

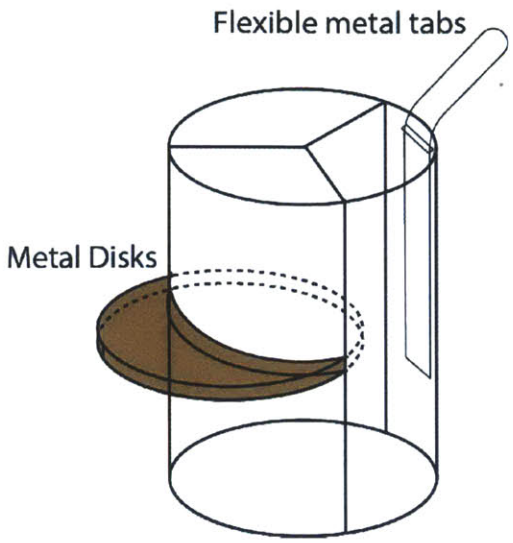

Figure 6-2: AREA INCREASING METHODS. This figure shows the two concepts to increase the area normal to the direction of tension from an anchor line. The first is a metal disk which can be extended outward from the device once it has burrowed to the desired depth. Three of these greatly increase the area. The second concept is a metal tab which can be extended from the top of the RoboClam. These could be a material which has a mechanical limit to how much it can bend. The tab could be pre-bent by a slightly curved slot as it leaves the RoboClam and when tension is put on the anchor line, the mechanical limits would prevent it from bending past a certain point.

6.1.3 Hydraulic Actuation

Hydraulic actuation could be used to move the RoboClam device for anchoring applications. With RoboClam 2, it is difficult to achieve high enough power density to move the device quickly enough for full fluidization. However, relocating the actuator away from the digging body could decrease the size of the part that digs, while allowing for a large actuator to generate the required power. Fig. 6-3 shows a schematic of this setup.

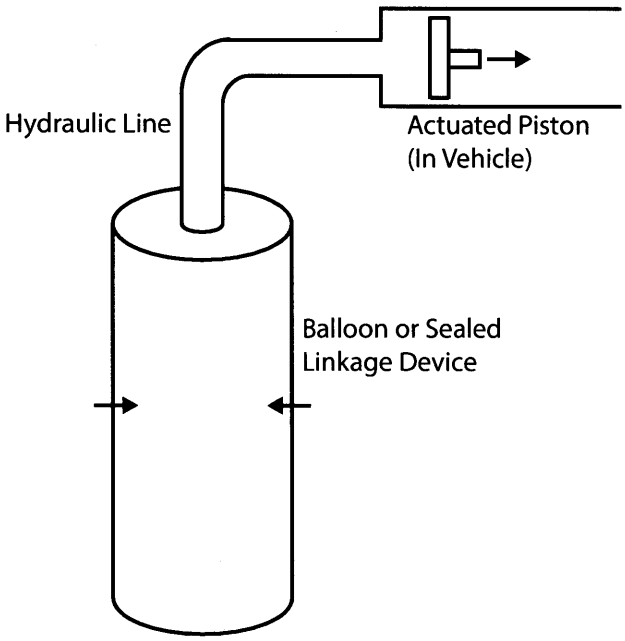

Figure 6-3: HYDRAULIC MOTION CONCEPT. This concept shows a method that could be used to actuate RoboClam for use on an underwater vehicle. The hydraulic actuator could be located inside the vehicle, and the hydraulic line would be used as a tether for the vehicle. This concept would increase the power density available and allow for relatively small anchors, as the power source would not be contained within the device.

Bibliography

[1] Kelly M. Dorgan, Peter A. Jumars, Bruce Johnson, B. P. Boudreau, and Eric Landis. Burrowing mechanics: Burrow extension by crack propagation. *Nature*, 433(7025):475–475, 02 2005.

[2] Ryan D. Maladen, Yang Ding, Chen Li, and Daniel I. Goldman. Undulatory swimming in sand: Subsurface locomotion of the sandfish lizard. *Science*, 325(5938):314–318, 07 2009.

[3] Meeting with bluefin robotics, June 2013.

[4] Personal obervation by the author, June 2011.

[5] A.F. Holland and J.M. Dean. The biology of the stout razor clam tagelus plebeius: I. animal-sediment relationships, feeding mechanism, and community biology. *Chesapeake Science*, 18(1):58–66, 1977.

[6] Amos G Winter V, Robin Deits, and Anette Hosoi. Localized fluidization burrowing mechanics of ensis directus. *Journal of Experiental Biology*, 215:2072–2080, 2012.

[7] Amos G. Winter and A. E. Hosoi. Identification and evaluation of the atlantic razor clam (ensis directus) for biologically inspired subsea burrowing systems. *Integrative and Comparative Biology*, 51(1):151–157, 07 2011.

[8] Amos Greene Winter, Robin Deits, Daniel Dorsch, Anette Hosoi, and Alexander Slocum. Teaching roboclam to dig: The design, testing, and genetic algorithm optimization of a biomimetic robot. pages 4231–4235. IROS, 2010.

[9] AG Winter, RLH Deits, DS Dorsch, AH Slocum, and AE Hosoi. Razor clam to roboclam: burrowing drag reduction mechanisms and their robotic adaptation. *Bioinspiration and Biomimetics*, 9(3):036009, 2014.

[10] Amos G Winter V. *Biologically inspired mechanisms for burrowing in undersea substrates.* PhD thesis, Massachusetts Institute of Technology, Cambridge MA, 2011.

[11] Daniel S Dorsch. The design of a fluidized bed for testing of a robotic burrowing device which mimics razor clams. Master's thesis, MIT, 2012.

[12] M.E. McCormick. *Anchoring Systems.* Oxford; New York, 1979.

[13] Daniel S. Dorsch and Amos G Winter. Design of a low energy, self contained subsea burrowing robot based on localized fluidization exhibited by atlantic razor clams. In *ASME IDETC*, number DETC2014-34953, 2014.

[14] Amos Winter V, Robin Deits, and D Dorsch. Critical timescales for burrowing in undersea substrates via localized fluidization, demonstrated by roboclam: A robot inspired by atlantic razor clams. In *Proceedings of IDETC/CIE 2013*, number 12798 in DETC2013, Aug 2013.

[15] Pijush K Kundu and Ira M Cohen. *Fluid Mechanics.* Elsevier Academic Press, 2004.

[16] P. K. Robertson and R. G. Campanella. Interpretation of cone penetration tests. part i: Sand. *Canadian Geotechnical Journal*, 20(4):718–733, 1983.

[17] R. C. Hibbeler. *Mechanics of Materials.* Prentice Hall, 4th edition, 2000.

[18] K. Terzagi, R. Peck, and G. Mesri. *Soil Mechanics in Engineering Practice.* Wiley-Interscience, 1996.

[19] Frank M. White. *Fluid Mechanics.* McGraw-Hill, 4th edition, 1998.

[20] *Technical Characteristics of Flexinol Actuator Wires.* Dynalloy Inc, 2015. `http://www.dynalloy.com/pdfs/TCF1140.pdf`.

[21] Linmot 2013. linear motor product datasheet. `http://www.linmot.com/fileadmin/doc/Overviews/Overview_Marketing_e_recent.pdf`.

[22] Coefficient of friction. In *Engineers Handbook*, 2006. `http://www.engineershandbook.com/Tables/frictioncoefficients.htm`.

[23] John Stanton. Friction coefficients for stainless steel (ptfe) teflon bearings. In *Wisconsin Highway Research Program*, 2010. `http://wisdotresearch.wi.gov/wp-content/uploads/WisDOT-WHRP-project-0092-08-13-final-report.pdf`.

[24] Smooth-on inc. 2015. `http://www.smooth-on.com/`.

[25] Amos G Winter V. Method and apparatus for penetrating particulate substrates., June 1, 2009. Patent application no. 12455392.